



ELSEVIER

Contents lists available at ScienceDirect

Engineering Failure Analysis

journal homepage: www.elsevier.com/locate/engfailanal

Influence of anisotropy on the cold bending of S600MC sheet metal

Iulian-Ionut Ailinei, Sergiu-Valentin Galatanu^{*}, Liviu Marsavina

Department of Mechanics and Strength of Materials, Politehnica University of Timisoara, Mihai Viteazu Bd., Timisoara 300222, Timis, Romania

ARTICLE INFO

Keywords:

Anisotropy
Digital image correlation
Finite element analysis
Cold forming

ABSTRACT

Metal sheet anisotropy is the directional dependence of mechanical properties. It is the key factor that must be considered when using numerical simulation to predict any manufacturing process that involves plastic deformation. The plastic strain ratio, also known as Lankford coefficients or R values, together with the forming limit curves (FLC), are industry standards for assessing the formability of sheet metals. Complete experimental data used in forming the simulation rarely exists. The current investigation focuses on obtaining material properties and verification data as inputs for cold-forming numerical simulation. Uniaxial tests are used to describe the stress-strain curves of the S600MC steel sheet in the rolling, diagonal and transverse direction. The 2D Digital Image Correlation (DIC) technique was used to capture surface strains more accurately than relying on the crosshead of the tensile machine. On the basis of the experimental tests results, an anisotropic model of material was constructed, which was later used as input data for a numerical model, which was later validated. An industry example is shown to emphasize how anisotropy affects the formability of metal sheet blanks. Therefore, a comparison between the physical part in the final shape and the results of the forming simulation has been achieved.

1. Introduction

Sheet metals demonstrate anisotropic plastic behavior due to crystallographic texture caused mainly by progressive rolling steps [1]. Cold bending of steel sheets is a widely used manufacturing process in the automotive industry due to its cost efficiency, and by avoiding line heating, the oxidative process of steel is thus avoided. The major application of sheet metal in the automotive industry includes doors, fenders, bumpers, roof panels, and seat frames [2–4]. The cold bending manufacturing process involves deformation of the sheet metal in the plastic range, followed by elastic unloading, deteriorating the properties of the material. One of the shortcomings of this process is the development of residual stress and strains that have the potential to reduce structural integrity and the useful life of the component. It is acknowledged that the plastic strain induced by cold bending reduces the material ductility, and the residual stresses lead to premature surface yielding, and both have the potential to reduce the fatigue life and have to be considered in the design limits.

During sheet metal, the rolling operation elongates and aligns the microstructure grains of the metal in the rolling direction and packs the grains in the thickness direction, leading to significantly different strength properties within the material. Lankford et al. (1950) [5] proposed a measure of plastic anisotropy of rolled metal sheets, by introducing plastic strain ratios, also called R values or Lankford values by the research community. These scalar quantities have been widely used in industry to assess the formability of

^{*} Corresponding author.

E-mail addresses: iulian.ailinei@student.upt.ro (I.-I. Ailinei), sergiu.galatanu@upt.ro (S.-V. Galatanu), liviu.marsavina@upt.ro (L. Marsavina).

Nomenclature

| | |
|--------------------------------------|--|
| $\sigma_0, \sigma_{45}, \sigma_{90}$ | Uniaxial tensile yield stress rolling direction (RD), in the tensile directions of 0° , 45° and 90° from rolling direction (RD) |
| $\sigma_{ij}, i, j = \{1, 2, 3\}$ | stress tensor components |
| $\bar{\sigma}$ | Effective stress |
| r_0, r_{45}, r_{90} | Lankford coefficients |
| σ_b | Yield stress under uniform biaxial tension |
| ϵ_w | Width strain |
| ϵ_l | Longitudinal direction strain |
| ϵ_t | Thickness strain |
| R | Normal anisotropy |
| Δr | Planar anisotropy |
| S_1, S_2 | Principal deviatoric stress |
| σ_1, σ_2 | Principal stresses |
| K_1, K_2 | Modified stress tensors |

recrystallized steel sheets by progressive rolling. Resistance to thinning can also be assessed on the basis of Lankford coefficients and is defined by the ratio of true strain in the width direction versus true strain in the thickness direction.

Design and analysis of cold-bending processes using empirical approaches implies a high cost of material and dies in trial-and-error procedures. Therefore, the numerical simulation of this process became particularly attractive. Numerical simulation of cold-forming processes needs a quantitative description of the plastic anisotropy; von Mises criteria is enough to describe yielding isotropic materials, but to consider anisotropy of the sheet metals, additional parameter has to be introduced.

Today's research is increasingly using Digital Image Correlation to examine full-field displacements and strain measurements of specimens subjected to different loads. A variety of applications are investigated using DIC. The evaluation of the mechanical shear response was investigated by Leitão [6], Pop [7] used DIC and FEM approaches to identify the mechanical state in the vicinity of a crack, Wang [8] used DIC system to measure the full-range strain distribution at the macroscopic level during a tensile test, a feature that is not available through conventional techniques, Falk [9] and [10] investigated the use of DIC and FEM for strain measurement on Printed Board Circuits. Barnefske [11] investigated an experimental comparison of fiber-bragg-grating (FBG) strain gauges, electrical strain gauges and the photogrammetric strain systems IView and ARAMIS in a tensile test. The sheet metal assessment using DIC was investigated by many researchers [12–14].

The first researcher who introduced the concept of quantification of the formability index, according to Banabic et al. [15], was Gensamer in 1946. He plotted the limit strains associated with each stress ratio on a rectangular diagram using the longitudinal and transverse principal strains as abscissa and ordinate, respectively. The curve thus obtained separates the area with acceptable strains (bellow the curve) from the area where defects, such as neck and fracture, occur. This concept was revised in the 1960s by Keeler [16] and published in a journal for a worldwide audience and was considered the first graphical representation of FLC. Goodwin in 1968 [15] extended the curve defined by Keeler into the negative strain domain.

FLC was widely accepted as the standard tool for studying the formability of sheet metals. Despite the fact that the FLC concept is simple to understand and apply, it has limitations. Plastic deformation depends on a large number of coupled effects that are difficult to predict even in a controlled environment such as testing facilities and makes the experimental determination of material failure nontrivial and time-consuming [17]. Furthermore, the scatter in the experimental data is so large that a statistical evaluation of the is of the measurement uncertainty needed [18]. These drawbacks motivated researchers to attempt to construct the limit curve of forming using theoretical and numerical methods.

The precision of the anisotropic yield criteria is the key to the accuracy of numerical simulations, either for a manufacturing process or assessment of the component's structural integrity. The objective of this paper is to characterize the evolution of plastic anisotropy for the S600MC steel sheet, used in the automotive industry, occupant safety.

In the first step, uniaxial tests were used to obtain the stress–strain curves of the S600MC steel sheet in the rolling, diagonal, and transverse directions. The DIC technique was used to capture full-field surface strains. Therefore, the stress–strain curves determined previously were used to build and validate the numerical model of the tensile specimens that were physically tested. In the end, an example from industry is shown to emphasize how anisotropy affects the formability of metal sheet blanks. A comparison between physical parts in final shape and the results of the forming simulation was achieved. For this study, the material parameters used in the forming simulation were based on the experimental and numerical models of the initial tensile tests.

2. Mathematical model

The concept of yield criterion for isotropic materials was introduced even before the curved forming limit concept by Richard Edler von Mises in 1924 [19]. He described that yielding of a ductile isotropic material begins when the second deviatoric stress invariant J_2 reaches a critical value.

Hill introduced a yielding criterion that accounts for anisotropy in 1948 [20], and it is simply an extension of the von Mises

criterion. Hill48 has a quadratic form. Predicts the same yield stress in tension and compression. Therefore, it cannot accurately describe the state of anisotropy in a way that is accurate enough even under stress conditions.

A modified version of Hill's yield criterion [21] is reported to be free of the shortcomings mentioned above, but does not contain the shear stress. Hill has the form:

$$\left(\frac{\sigma_1}{\sigma_0}\right)^2 + \left(\frac{\sigma_2}{\sigma_{90}}\right)^2 + \left[p + q - c - \frac{p\sigma_1 + q\sigma_2}{\sigma_b}\right] \left(\frac{\sigma_1\sigma_2}{\sigma_0\sigma_{90}}\right) = 1 \tag{1}$$

where p, q, c, are non-dimensional parameter and σ_1, σ_2 are the principal stresses.

Hershey introduced a different class of yielding criteria based on crystal plasticity in 1954 [22], and was valued by Hosford in 1972, by developing its anisotropic criterion [23]. Hosford72 has the form:

$$F|\sigma_{22} - \sigma_{33}|^a + G|\sigma_{33} - \sigma_{11}|^a + H|\sigma_{11} - \sigma_{22}|^a = \sigma^a \tag{2}$$

where F, G, H are constants that must be determined experimentally, and σ_{ij} are the stresses.

The essential difference between the approaches of Hosford and Hill consists of the different ways of determining exponent a. Hosford was related to the crystallographic structure of the material. The drawback of this criterion is that it misses shear stress, so it cannot predict planar anisotropy.

Barlat developed an entire family of yield criteria, by progressive improving the Hosford approach. Together with Lian, he proposed in 1989 [24] a nonquadratic yield criterion, known as Barlat89, that included a shear stress member and was applicable for the three-dimensional plane stress case, assumed in sheet metal forming.

$$\alpha|K_1 + K_2|^m + \alpha|K_1 - K_2|^m + (2 - \alpha)|K_2^m| = 2\sigma^{-m} \tag{3}$$

$$K_1 = \frac{\sigma_{xx} + \sigma_{yy}}{2} \tag{4}$$

$$K_2 = \sqrt{\left(\frac{\sigma_{xx} + h\sigma_{yy}}{2}\right)^2 + p_2\sigma_{xy}^2} \tag{5}$$

where K1 and K2 were modified stress tensors, α, h, p and m are material constants and σ was effective stress.

Among the advantages, Barlat89 has only four parameters that are relatively easy to identify, except parameter p, which can only be numerically evaluated by solving a non-linear equation. In addition, it cannot give an accurate prediction of the biaxial yield stress. Despite its disadvantages, it is still popular among numerical simulations of sheet metal forming processes.

To overcome these disadvantages, in 1992, Barlat [25] proposed an extension of the previous criterion, increasing the number of parameters to six, allowing its usage to any stress [23]. In 2003 another yield stress function was described by Barlat et al. [26], known as Yld2000-2d, specifically for plane stress cases (2D). Compared to the Barlat-91 yield stress function, the Yld2000-2d function has eight anisotropic coefficients that are related to experimental yield stresses ($\sigma_0, \sigma_{45}, \sigma_{90}$) and anisotropies (r_0, r_{45}, r_{90}, r_b) obtained from samples prepared in different directions.

$$\Phi = \Phi' + \Phi'' = 2\sigma^a, \tag{6}$$

$$\Phi' = |S_1 - S_2|^a \tag{7}$$

$$\Phi'' = |S_1 + 2S_2|^a + |2S_1 + S_2|^a \tag{8}$$

S_1 and S_2 are the main deviatoric stresses; a is a parameter experimentally determined that characterizes the crystallographic structure of the material [23]. After linear transformation and writing the equations in Cauchy tensor terms, there are eight terms. Therefore, eight material characteristics are needed to express his function.

Using a similar approach, Barlat proposed in 2005 [27], a 3D yield criterion, known in the research community as Yld2004-18p, and has the form:

$$\Phi = |s_1' - s_1''|^a + |s_1' - s_2''|^a + |s_1' - s_3''|^a + |s_2' - s_1''|^a + |s_2' - s_2''|^a + |s_2' - s_3''|^a + |s_3' - s_1''|^a + |s_3' - s_2''|^a + |s_3' - s_3''|^a = 4\sigma^a \tag{9}$$

In order to identify all coefficients, the uniaxial yield stress and anisotropy coefficients in seven directions in the sheet plane ($0^\circ, 15^\circ, 30^\circ, 45^\circ, 60^\circ, 75^\circ$, and 90° with respect to the rolling direction) and four additional out-of-plane yield stresses were considered. This model is capable of accurate predictions in in-plane variation of the uniaxial yield stress and the coefficient of planar anisotropic but is not always suitable in practical applications due to the complexity of the formulation and the need of crystal plasticity models that are mandatory to evaluate some parameters. Yld2004-18p is implemented in LS-Dyna, commercial finite element code [23].

Banabic and his research team have made substantial experimental and numerical advances in the field of sheet metal anisotropy. The first formulation for the Banabic-Balan-Cazacu (BBC) yield criteria family was proposed in 2000 [28], incorporated the advantages of the Barlat criteria mentioned above, and by adding weighted coefficients, the resulting criterion was more flexible. BBC-2000 has the following form:

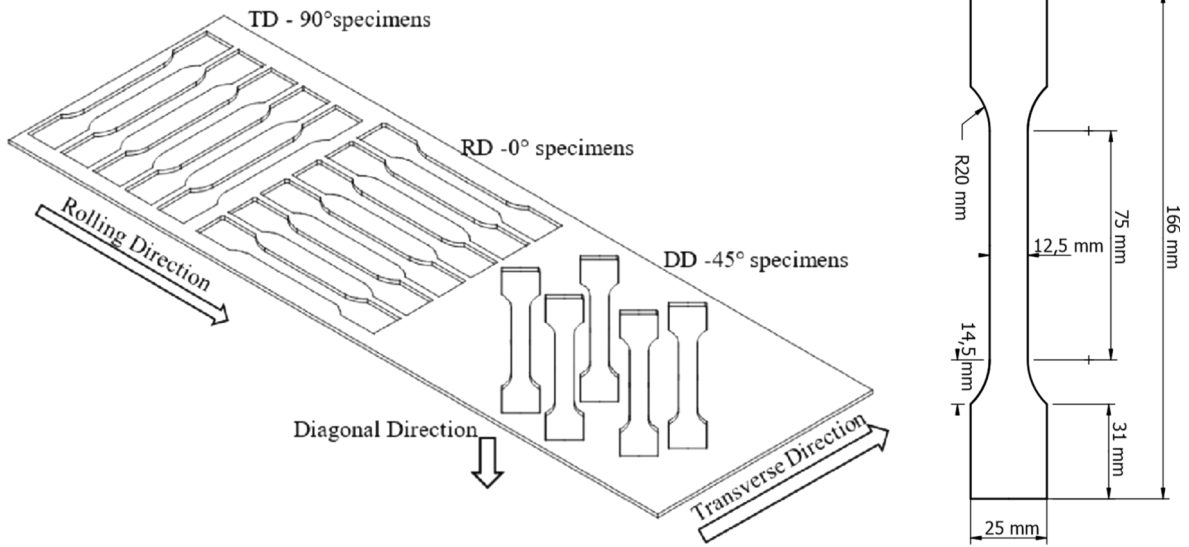


Fig. 1. a) Test specimen orientation on sheet metal blank and b) Dimensions of the specimens according to the ISO 10113:2006 standard [32].

$$\bar{\sigma} = [a(b\Gamma + c\Psi)^{2k} + a(b\Gamma - c\Psi)^{2k} + (1 - a)(2c\Psi)^{2k}]^{\frac{1}{2k}} \tag{10}$$

where a, b and k are material parameters, while Γ and Ψ second and third invariants of the transformed stress tensor. Banabic et al. [29], proposed an improvement of this model to account for an additional parameter, namely the biaxial anisotropy coefficient. BBC-2003 has the form:

$$\bar{\sigma} = [a(\Gamma + \Psi)^{2k} + a(\Gamma - \Psi)^{2k} + (1 - a)(2\Lambda)^{2k}]^{\frac{1}{2k}} \tag{11}$$

$$\Gamma = \frac{\sigma_{11} + M\sigma_{22}}{2} \tag{12}$$

$$\Psi = \sqrt{\frac{N\sigma_{11} - P\sigma_{22}^2}{2} + Q^2\sigma_{12}\sigma_{21}} \tag{13}$$

$$\Lambda = \sqrt{\frac{R\sigma_{11} - S\sigma_{22}^2}{2} + T^2\sigma_{12}\sigma_{21}} \tag{14}$$

where $k \in \mathbb{N} \geq 1$ and $0 \leq a \leq 1$, M, N, P, Q, R, S, and T are material properties; Γ , Ψ , and Λ are functions that depend on the planar components of the stress tensor.

Although the yield function has simple expressions and can accurately describe the yield surface, its coefficients have no physical meaning, the formulation of the yield criterion is not user-friendly, and the extension to 3D is not trivial. The BBC2003 yield criterion is reducible both to Hill 1948 and Barlat 1989 formulations. Furthermore, Barlat et al. [30] showed that BBC2003 and Barlat 2000 are the same, although the development procedures are different: the Banabic-Balan-Cazacu family emerged by adding coefficients to the classical Hershey formulation, while the Barlat family uses linear transformation. The linear transformation procedure is computationally expensive, making the BBC family the preferred choice when numerical simulations of sheet metal forming are employed. A modified version of this criterion, BBC 2005 [29], is implemented in the AutoForm 4.1 commercial finite element program [23]. To improve the flexibility of the previous, the BBC 2008 model version [31] was proposed. This model uses changeable input values expressed as finite series that can expand or contract to retain as many terms as available from the experimental data. Because of this, BBC2008 maintains superior computational efficiency by avoiding the linear transformation of the stress tensor.

The interest in the field is proven by the extensive research work available, but at the same time, the state-of-the-art in this field is also confusing since all the criteria listed above (and many other developments based on the principal classes) are still employed in the actual design and analysis phase. The flexibility of the criterion, the robustness of the identification procedure, experimental difficulties caused by the determination of the mechanical parameters involved in the identification procedure, and computational should be considered when choosing the yield criterion in the industrial application.

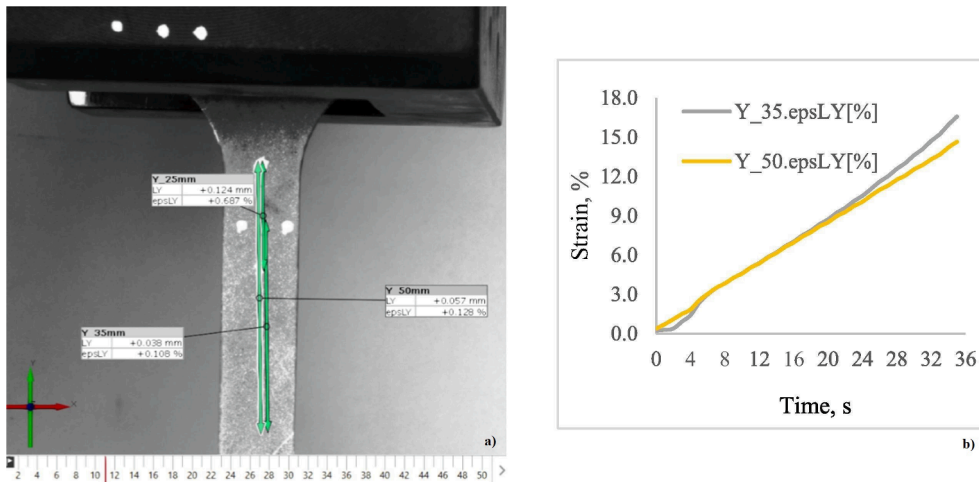


Fig. 2. Virtual Extensometer: a) GOM graphical user interface and b) output examples.

3. Materials and methods

3.1. Material characterization

The anisotropy characterization was developed and analyzed considering the directional dependencies of the properties of the plastic material obtained in the uniaxial tensile tests for 3.0 mm thick S600MC sheet metal. Tensile test specimens were laser cut at orientations $\theta = 0^\circ$, 45° , and 90° with respect to the rolling direction as shown in Fig. 1a.

Four tensile specimens were tested for each orientation. The geometry of specimens with a 12.5 mm wide and 75 mm long gauge section follows ISO 10113:2006 standard. The specimen geometry specifications are depicted in Fig. 1b.

Digital Image Correlation (DIC) is a noncontact optical deformation measuring technique used to capture full-field material strain. A series of time-lapse photographs were captured by Aramis 2D SRX GOM (2013b) DIC equipment developed by GOM. The images were captured while the test specimens (device under test-DUT) were loaded in tension. Before the image capturing process, the DUTs were sprayed with non-reflective dull white paint, and then, after curing, black paint droplets were applied. The spraying process aims to generate a stochastic pattern on the DUT, with the size of the speckles of 0.5–3 mm. To analyze the deformation of the specimen, the corresponding picture points in any picture were measured. A grid with a facet size of 19×19 pixels summarizes the picture point measurements. Each facet overlaps its neighbors by 21%. The points are identified in each consecutive image and their positions are assigned with subpixel accuracy. The accuracy can be reached up to 10–50 $\mu\text{m}/\text{m}$. The software can determine the displacements of the points, and their velocity and acceleration caused by the load. In addition, the surface software can control the deformation of the test object by creating a map of major or minor deformations [33].

An LBG TC100 universal testing machine was used to perform the uniaxial tensile test. The loading conditions (strain rate) have been chosen to meet the ISO 10113:2006 standard. Tests were performed at room temperature.

Virtual extensometer locations were chosen during post processing of the test results, and they were placed in the gauge section of the specimen but outside the neck area, where strain localization is expected.

To generate the stress–strain curves, the force signal from LBG TC100 was combined with the deflection measured by DIC. Then, based on the force displacement curves generated in this way, the engineering curves and the true stress strain curves were computed.

To ensure measurement redundancy, three virtual extensometers were used for all tensile specimens, Fig. 2a and the output results shown in Fig. 2b.

3.2. Lankford coefficients determination by DIC

The crystal structure after cold rolling of the sheet metal leads to anisotropic behavior. The anisotropy of plastic behavior is computed using the Lankford coefficients [5] following ISO 10113-2006 [32]. Plastic strain ratios were manually determined based on tensile tests and DIC, performed previously. The plastic strain ratio, r , was determined first, which is the ratio of the true width strain to the true thickness strain of a test piece subjected to uniaxial tensile stress. Since it is much easier to measure the change in length than in thickness, based on the law of constancy of volume, the following relationship was used to compute the plastic strain ratio for all three orientations.

$$r = \frac{\ln\left(\frac{b}{b_0}\right)}{\ln\left(\frac{L_0 b_0}{L b}\right)} \quad (15)$$

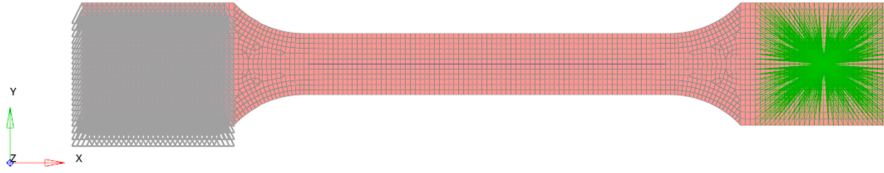


Fig. 3. FEA model of the tensile specimen.

The weighted average of the plastic strain ratio, \bar{R} , shows the difference between the mechanical properties measured in-plane and through thickness, and this gives the measure of anisotropy.

$$\bar{R} = \frac{r_0 + r_{90} + 2r_{45}}{4} \quad (16)$$

For isotropic materials, the \bar{R} value is equal to 1. A higher \bar{R} value shows that through thickness strength is greater than in-plane strength, which leads to higher formability of the steel.

The degree of planar anisotropy was computed next, based on the relationship:

$$\Delta r = \frac{r_0 + r_{90} - 2r_{45}}{2} \quad (17)$$

Based on determined Lankford coefficients, the anisotropic state of material can be described by computing the constants that are part of Hill, Barlat, or Banabic anisotropic yield criteria families, and inputted in Finite Element Solvers.

3.3. Finite element analysis

Numerical investigations were divided into two parts. The stress–strain curves determined previously were used to build and validate numerical models of the tensile specimens that were physically tested. The results obtained initially from the material validation were used to build the forming limit curve and used in the forming simulation.

3.3.1. Material model

The mechanical properties of the S600 MC sheet metal were determined through tensile tests in three directions with respect to the rolling directions. The elastic behavior was considered in the numerical simulations by the value of Young's modulus, $E = 210\,000$ MPa and the Poisson's ratio, $\nu = 0.3$. The isotropic hardening behavior was modeled using a power-law type, using the Holomon expression [34]:

$$\sigma = C\varepsilon^n \quad (18)$$

where C is a material constant, and n is the strain-hardening exponent.

The behavior of plastic material was numerically modelled by the von Mises yield criterion (Eq. (19)) and Hill's 1948 (Eq. (20)) to take into account the anisotropy condition.

$$\sigma_v = \sqrt{3J_2} = \sqrt{\frac{(\sigma_{11} - \sigma_{22})^2 + (\sigma_{22} - \sigma_{33})^2 + (\sigma_{33} - \sigma_{11})^2 + 6(\sigma_{12}^2 + \sigma_{23}^2 + \sigma_{31}^2)}{2}}$$

$$\sigma_v = \sqrt{\frac{(\sigma_1 - \sigma_2)^2 + (\sigma_2 - \sigma_3)^2 + (\sigma_3 - \sigma_1)^2}{2}} = \sqrt{\frac{3}{2} s_{ij} s_{ij}} \quad (19)$$

$$F(\sigma_{22} - \sigma_{33})^2 + G(\sigma_{33} - \sigma_{11})^2 + H(\sigma_{11} - \sigma_{22})^2 + 2L\sigma_{23}^2 + 2M\sigma_{31}^2 + 2N\sigma_{12}^2 = 1 \quad (20)$$

where F , G , H , L , M , N are constants that must be determined experimentally, and σ_{ij} are the stresses. It predicts the same yield stress in tension and compression.

The previously determined stress–strain curves were used to build numerical simulation models of the tensile specimens that were physically tested. The geometry of the test specimen was meshed with first-order hexahedral elements, with an average size of 1 mm; three elements per thickness were used to ensure the proper stress gradient. The model was constrained at one end, 0 degree of freedom (left side of the specimen) and subjected to enforced in-plane displacement, along the X axis, as depicted in Fig. 3. All the nodes from the right side of the specimen that are clamped in the vices of the tensile equipment, were connected via a rigid body element (RBE2). A 20 mm displacement was imposed on the RB pilot node. By using the Altair Optistruct FEA structural analysis solver, a nonlinear elasto-plastic, quasi-static simulation was performed, with the aim to have validated the numerical models of the tensile tests performed previously.

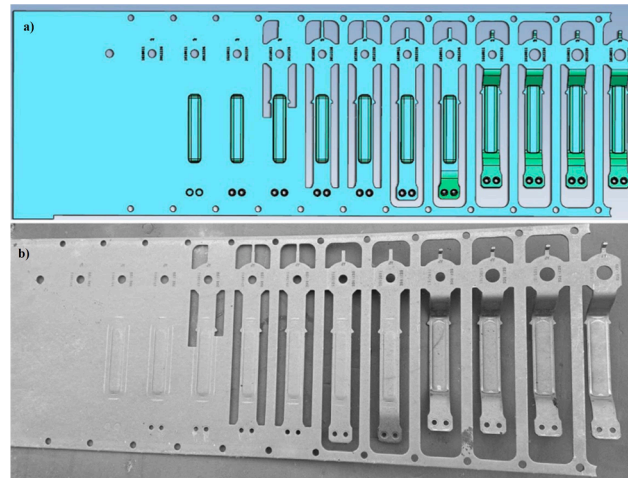


Fig. 4. Progressive die forming of the seatbelt bracket: a) CAD model and b) actual progressive sheet metal.

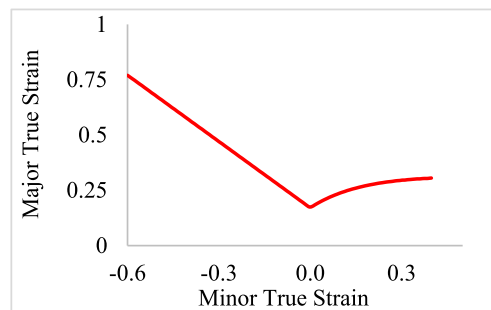


Fig. 5. Forming Limit Curve of S600 steel.

3.3.2. Numerical analysis of the seatbelt bracket forming

Progressive die stamping is a highly employed metalworking process in the automotive industry. Usually combined with an automatic feeding system, it is a highly productive manufacturing process suitable for the mass production of sheet metal parts having complex geometries. A feeding system unrolls a sheet metal from a coil and pushes it through a series of stations that progressively deform the raw material, in multi-stages, by bending, punching, coining, or other operations, until the finished part is obtained. Several centering holes in the metal strip driven by conical or round ‘pilots’ are part of the precision of the system that ensure the required length during the advance of the blank metal at the processing stages. The seatbelt bracket in the discussion can be seen in Fig. 4, from the raw material (left) to the final shape (right) right before the final cutoff operation, where the finished product is separated from the rest of the sheet metal webbing.

The forming simulation aims to assess the feasibility of the progressive die forming of a safety component used in the automotive industry. The bracket mechanically connects the seatbelt assembly to the car chassis. The seatbelt bracket is subjected to static, vibrating, and dynamic nonlinear loads during its working life. According to the applicable occupant safety standards, this component should maintain its structural integrity during all crash scenarios and should not break under a load of less than 20kN. For these reasons, including a robust numerical simulation of the forming process, doubled by material characterization, is crucial for a robust design process.

For the stamping simulation, Altair Inspire Form was employed to check the formability of a part early in the product design cycle. Potential defects such as splits or wrinkles can be identified and modified to improve the overall design. Part geometry, material parameters and manufacturing process parameters were considered inputs for this analysis. For the forming simulation Barlat yield criterion was used. The strength coefficient and strain hardening were obtained experimentally.

The final shape, part after the stamping process, was imported into the Inspire Form preprocessor. The first step was to extract the middle surface of the solid sheet metal geometry. The resulting mid-surface was meshed with 0.5 mm shell elements (quads and shells).

The material behavior for the stamping simulation was described by the elastic–plastic and anisotropy parameters (R-values) previously determined by physical tests. The forming limit curves for this S600MC steel were raised, shown in Fig. 5.

Process parameters such as stamping direction and blank-holder constraints were specified to replicate physical manufacturing. The blank holder applies a predefined force to control material flow into the die cavity and was set at 10 kN. The blank holder is only a numerical constraint in this simulation, not shown. A friction coefficient of 0.1 was defined between the blank holder and the sheet

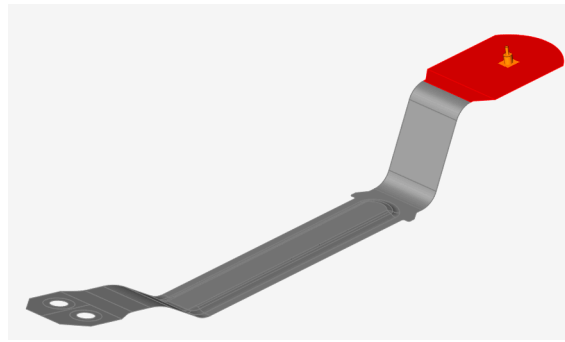


Fig. 6. Simulation model of the seatbelt bracket.

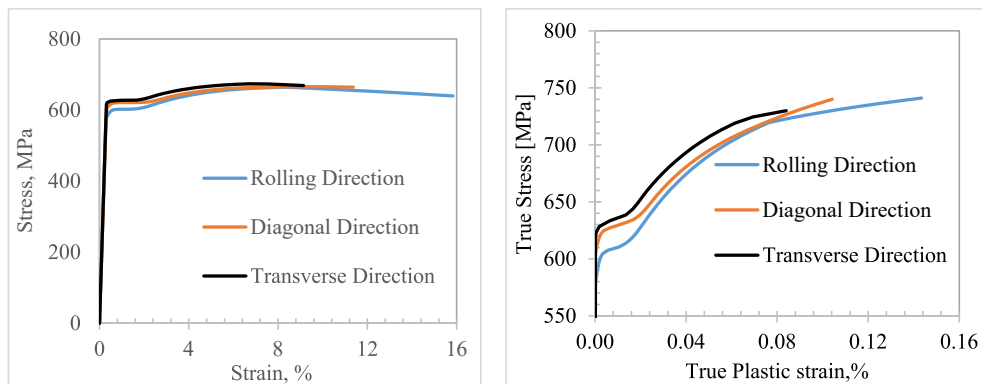


Fig. 7. a) Engineering stress–strain curves and b) true stress–true plastic strain curves for S600MC steel, in rolling, diagonal, and transverse directions.

Table 1

Principal properties at different orientations and Lankford coefficients for S600MC steel.

| Orientation, θ | Specimens no. | YS[MPa] | \overline{YS} [MPa] | \overline{US} [MPa] | r | R | Δr | C [MPa] | n |
|------------------------------|------------------|---------|-----------------------|-----------------------|------|-------|------------|------------|--------|
| 0°- Rolling Direction | 1 | 647.75 | 621.35 | 747.50 | 1.17 | 1.138 | 0.12 | 861.6 | 0.0590 |
| | 2 | 605.61 | | | | | | | |
| | 3 | 577.09 | | | | | | | |
| | 4 | 655.05 | | | | | | | |
| 45°- Diagonal Direction | 1 | 652.98 | 635.78 | 740.97 | 1.13 | | | 835.5 | 0.0498 |
| | 2 | 623.40 | | | | | | | |
| | 3 | 657.45 | | | | | | | |
| | 4 | 626.51 | | | | | | | |
| 90°- Transverse Direction | 1 | 608.31 | 599.08 | 698.92 | 1.10 | | | 784.1 | 0.0483 |
| | 2 | 584.01 | | | | | | | |
| | 3 | 607.52 | | | | | | | |
| | 4 | 596.51 | | | | | | | |

metal part. A clamping for 10kN holds the sheet. In Fig. 6 simulation model with constraints is shown.

4. Results and discussion

The engineering stress–strain curve was obtained from the conventional uniaxial tensile test. Engineering strain is defined by the uniaxial deformation relative to the initial gauge length L_0 . Engineering stress is defined by dividing the load by the initial cross-section area. In Fig. 7a are plotted the results obtained for engineering stress–strain curve along rolling (RD), diagonal (DD) and transversal direction (TD) respectively.

It can be seen that, at the beginning, the deformation is very small and the specimen is elastic. In this area, there is a linear relationship between engineering stress and the engineering strain. The engineering stress increases linearly with increasing

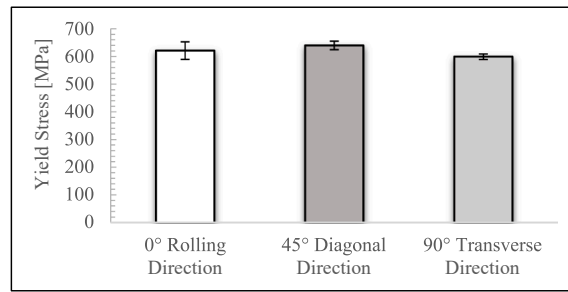


Fig. 8. The orientation dependency of Yield Stress.

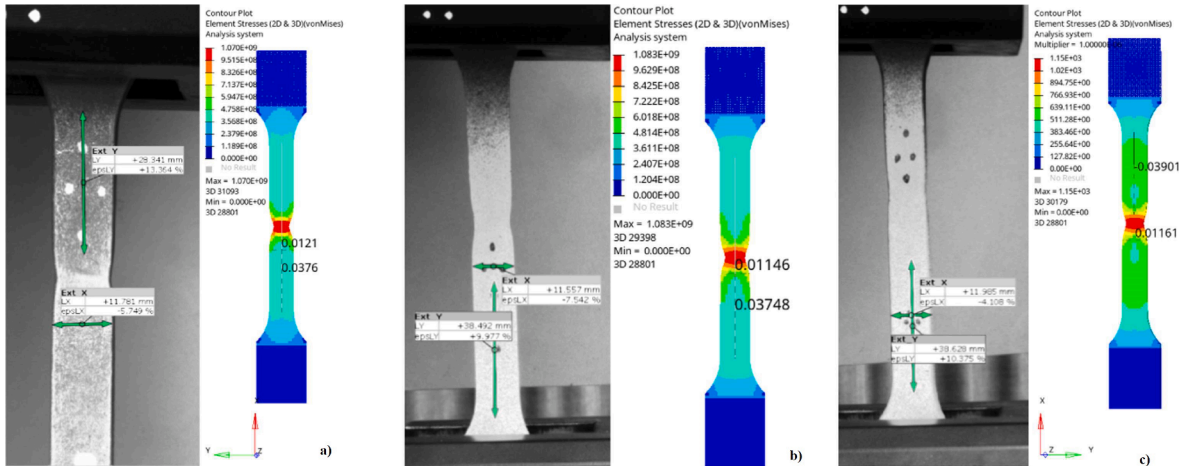


Fig. 9. Tests vs numerical analysis: a) RD, b) DD and c)TD.

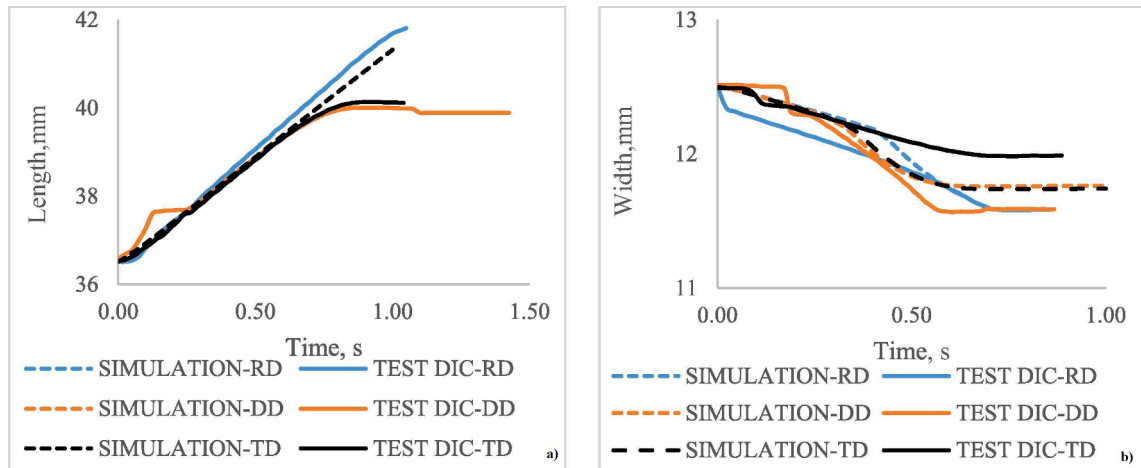


Fig. 10. FEA simulation vs physical test evaluated by Digital image correlation: a) change in length, and b) change in width of the test specimens.

engineering strain in the elastic regime and ends when the specimen enters the plastic domain. After the specimen goes to the plastic domain, this region is known as yielding. The elastic part and the yielding take place in the early stage of the whole deformation of the specimens. After yielding, the engineering stress increases with increasing engineering strain. This part is known as strain hardening. After reaching the maximum engineering stress, plastic instability and flow localization will occur just after the maximum load and the so-called diffuse necking starts. The maximum engineering stress is known as the ultimate tensile stress, and the corresponding engineering strain is called the uniform elongation. After the onset of diffuse necking, the deformation is located in the necking zone. A

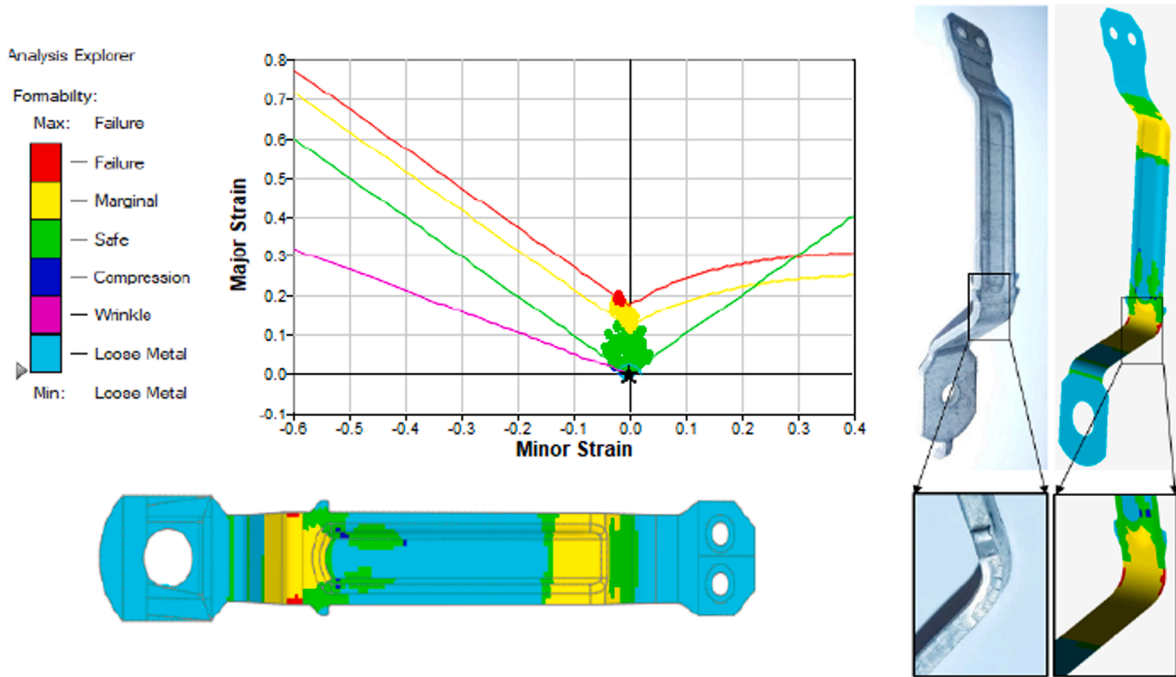


Fig. 11. a) Formability of S600 steel bracket and b) FEA versus physical part.

sudden drop in engineering stress can be observed when the specimen breaks apart. At this stage, the data obtained from the extensometer are no longer valid, since the uniaxial deformation assumption does not stand [35].

Taking into account engineering stress–strain curve, the true stress–true plastic strain curve for S600 steel along RD, DD and TD, respectively, was plotted, Fig. 7b.

In Table 1 are presented the principal properties at different orientations and the Lankford coefficients for the S600MC steel. Yield stress (YS) is calculated with the offset method by drawing a parallel line to the elastic part of the stress–strain curve that intersects the abscissa at 0.2%. Ultimate stress (US) is the maximum value of the ordinate from the true stress–plastic strain curve. The variation of the yield stress and the ultimate stress shown in Table 1 is below 5%. Lankford coefficients were obtained using equations (15), 16 and 17.

The orientation dependency of Yield Stress is presented in Fig. 8.

The previously determined stress–strain curves were used to build numerical simulation models of the tensile specimens that were physically tested along rolling (RD), diagonal (DD) and transversal direction (TD) respectively. A capture from the experimental test and numerical simulation side by side comparison are presented in Fig. 9.

A good correlation between the results obtained from FEA simulation versus the physical tests evaluated by DIC was observed for the change in length and width of the test specimens. The results are presented in Fig. 10.

The principal strain on the surface of the sheet metal is plotted against the forming limit curve of the material, to identify deformation areas that occurred in the forming process, Fig. 11a. Color coding is used to indicate the potential for failure due to excessive deformation during the cold bending process, or the areas where the material is highly compressed, tends to wrinkle, or is not sufficiently deformed. The red color indicates a high potential for failure because the minor and major strain are higher than the FLC curves. The yellow color indicates some potential for failure during forming of the components. The green color indicates the safety zone of the components, without potential to exceed the strain limits. Blue color indicates that the parts are loaded in compression. Magenta color indicates another failure mechanism, which is wrinkling during the manufacturing process. Wrinkling is the excessive compressive deformation of the material beyond its limits. The turquoise color indicates that the material is not sufficiently deformed during forming.

Fig. 11b shows a comparison between the physical part in the final shape and the forming simulation results. Simulation results show that the vast majority of the part is not loaded, and the metal is loose, depicted in turquoise. In the model, there is no potential for wrinkling, as the area covered in magenta is not present. As expected, in the radii regions green and yellow colors are present. The green color shows good formability of the bracket and the material is stretched almost to the material's limits as depicted by the yellow color.

One can observe that the cracks that occur in the bending radii of the physical part match the red elements in the FEA model that are above the FLC of the material, suggesting that the numerical model correctly predicted the formability of the S600MC steel bracket.

5. Conclusions

In this study anisotropy investigation of S600MC steel was shown, using physical testing, digital image correlation, and finite element modeling.

The rolling process causes anisotropy in sheet metals. Anisotropy in sheet metal is quantified by performing uniaxial tensile on test specimens milled in rolling, diagonal, and transverse directions. Using DIC method the stress–strain curve for the three different direction was measured. The variation of the yield stress and the ultimate stress obtained are below 5%. As expected there is an orientation dependency of the yield and ultimate stresses. After the uniaxial tensile tests were performed a numerical correlation was achieved in order to validate and verify the material model. The resulting material model with the Lankford parameters and an anisotropic yield criteria were used as inputs for the numerical simulation of the forming process, conducted with an explicit FEA solver.

To predict the formability of the metal by numerical methods, material models must rely on extensive physical testing. This study shows an experimental method to obtain the parameters used in the forming process simulation. The failure criteria Barlat [24], embedded in the explicit solver Altair Inspired Form, give the same location of the neck and failure point and correlate with physical parts.

Future work will focus on analyzing the influence of anisotropy and permanent plastic strain on vibrational fatigue and impact loads.

Declaration of Competing Interest

The authors declare that they have no known competing financial interests or personal relationships that could have appeared to influence the work reported in this paper.

Acknowledgements

The project leading to this application has received funding from the European Union's Horizon 2020 research and innovation program under grant agreement No 857124.

References

- [1] D. Banabic, H.-J. Bunge, K. Pöhlndt, A. E. Tekkaya, Formability of Metallic Materials, Springer-Verlag, Print ISBN: 978-3-642-08750-9, Electronic ISBN: 978-3-662-04013-3, 2000.
- [2] S. Sulaiman, M.K.A.M. Ariffin, S.Y. Lai, Springback behavior in sheet metal forming for automotive door, AASRI Procedia 3 (2012) 224–229, <https://doi.org/10.1016/j.aasri.2012.11.037>.
- [3] F. Claus, B. Hamann, H. Leitte, H. Hagen, Decomposing deviations of scanned surfaces of sheet metal assemblies, J. Manuf. Syst. 61 (2021) 125–138, <https://doi.org/10.1016/j.jmsy.2021.08.011>.
- [4] B. Chongthairungruang, V. Uthaisangsk, S. Suranuntchai, S. Jirathearanat, Springback prediction in sheet metal forming of high strength steels, Mater. Des. 50 (2013) 253–266, <https://doi.org/10.1016/j.matdes.2013.02.060>, September.
- [5] W.T. Lankford, S.C. Snyder, J.A. Bauscher, New criteria for predicting the press performance of deep drawing sheets, Trans. ASM 42 (1950) 1197–1205.
- [6] C. Leitão, M.I. Costa, D.M. Rodrigues, Assessment of mechanical shear response using digital image correlation, Revista da Associação Portuguesa de Análise Experimental de Tensões, ISSN 1646-7078, 2014.
- [7] Octavian Pop, Mamadou Meite, Frédéric Dubois, Joseph Absi, Identification algorithm for fracture parameters by combining DIC and FEM approaches, Int. J. Fract. 170 (2) (2011) 101–114, <https://doi.org/10.1007/s10704-011-9605-y>.
- [8] Y.H. Wang, J.H. Jiang, C. Wanintrudal, C. Du, D. Zhou, L.M. Smith, L.X. Yang, Whole field sheet-metal tensile test using digital image correlation, Exp. Tech. 34 (2) (2010) 54–59, <https://doi.org/10.1111/j.1747-1567.2009.00483.x>.
- [9] A. Falk, L. Marsavina, O. Pop, Analysis of Printed Circuit Boards strains using finite element analysis and digital image correlation, Frattura ed Integrità Strutturale 51 (2020) 540–551, <https://doi.org/10.3221/IGF-ESIS.51.41>.
- [10] A. Falk, L. Marsavina, O. Pop, Experimental determination of strain distribution on Printed Circuit Boards using Digital image correlation, Procedia Structural Integrity 18 (2019) 214–222, <https://doi.org/10.1016/j.prostr.2019.08.156>, 2019.
- [11] E. Barnefske, F. Keller, C. Gehmert, H. Sternberg, H. Sternberg, A Comparison of Strain Measurement Systems in a Tensile Experiment, Conference: FIG Working Week, Christchurch, New Zealand, May 2–6, 2016.
- [12] G.B. Broggiato, D. Ferrari, M. Fischer, V. Veglianti, Sheet-metal assessment at medium strain-rates by digital image correlation, Strain 46 (2010) 396–403, <https://doi.org/10.1111/j.1475-1305.2009.00668.x>.
- [13] M. Sasso, M. Rossi, G. Chiappini, G. Palmieri, Sheet Metals Testing with Combined Fringe Projection and Digital Image Correlation, Proceedings of XII SEM Annual Conference, 2016-11-18T14:43:06Z, 2019.
- [14] V.T. Nguyen, S.J. Kwon, O.H. Kwon, Y.S. Kim, Mechanical properties identification of sheet metals by 2D-digital image correlation method, Procedia Eng. 184 (2017) 381–389, <https://doi.org/10.1016/j.proeng.2017.04.108>.
- [15] Dorel Banabic, Abdolvahed Kami, Dan-Sorin Comsa, Philip Eyckens, Developments of the Marciniak-Kuczynski model for sheet metal formability: a review, J. Mater. Process. Technol. 287 (2021) 116446, <https://doi.org/10.1016/j.jmatprotec.2019.116446>.
- [16] S. Keeler, Plastic instability and fracture in sheet stretched over rigid punches, Trans. Am. Soc. Met. 56 (1963) 25–48.
- [17] B. Mohammed, T. Park, H. Kim, F. Pourboghrat, R. Esmailpour, The forming limit curve for multiphase advanced high strength steels based on crystal plasticity finite element modeling, Mater. Sci. Eng. 725 (2018) 250–266, <https://doi.org/10.1016/j.msea.2018.04.029>, 16 May.
- [18] K. Janssens, F. Lambert, S. Vanrostenberghe, M. Vermeulen, Statistical evaluation of the uncertainty of experimentally characterised forming limits of sheet steel, J. Mater. Process. Technol. 112 (2–3) (2001) 174–184, [https://doi.org/10.1016/S0924-0136\(00\)00890-6](https://doi.org/10.1016/S0924-0136(00)00890-6), 25 May.
- [19] R. von Mises, *Mechanik der festen Körper im plastisch-deformablen Zustand*, Nachrichten von der Gesellschaft der Wissenschaften zu Göttingen. Mathematisch-Physikalische Klasse, vol. 4, pp. 592–582, 1913.
- [20] R. Hill, A theory of the yielding and plastic flow of anisotropic metals, 27 May 1948, vol. 193, no. 133, 1948.
- [21] R. Hill, User-friendly theory of orthotropic plasticity in sheet metals, Int. J. Mech. Sci. 35 (1) (1993) 19–25, [https://doi.org/10.1016/0020-7403\(93\)90061-X](https://doi.org/10.1016/0020-7403(93)90061-X).
- [22] A. Hershey, The plasticity of an isotropic aggregate of anisotropic face centered cubic crystals, J. Appl. Mech. 21 (1954) 241–249, <https://doi.org/10.1115/1.4010900>.

- [23] D. Banabic, Plastic behavior of sheet metals, in: *Sheet Metal Forming Process*, Berlin, Heidelberg, Springer, 2010, pp. 27-140.
- [24] F. Barlat, K. Lian, Plastic behavior and stretchability of sheet metals. Part I: A yield function for orthotropic sheets under plane stress conditions, *Int. J. Plast.* 5(1) (1989) 51-66, [https://doi.org/10.1016/0749-6419\(89\)90019-3](https://doi.org/10.1016/0749-6419(89)90019-3).
- [25] F. Barlat, D.J. Lege, J.C. Brem, A six-component yield function for anisotropic materials, *Int. J. Plast.* 7 (7) (1991) 693-712, [https://doi.org/10.1016/0749-6419\(91\)90052-Z](https://doi.org/10.1016/0749-6419(91)90052-Z).
- [26] F. Barlat, J.C. Brem, J.W. Yoon, K. Chung, R.E. Dick, D.J. Lege, F. Pourboghra, S.H. Choi, E. Chu, Plane stress yield function for aluminum alloy sheets—part 1: theory, *Int. J. Plast.* 19 (9) (2003) 1297-1319, [https://doi.org/10.1016/S0749-6419\(02\)00019-0](https://doi.org/10.1016/S0749-6419(02)00019-0), September.
- [27] F. Barlat, H. Aretz, J.W. Yoon, M.E. Karabin, J.C. Brem, R.E. Dick, Linear transformation-based anisotropic yield functions, *Int. J. Plast.* 21 (5) (2005) 1009-1039.
- [28] D. Banabic, T. Balan, D.S. Comsa, A new yield criterion for orthotropic sheet metals under plane-stress conditions, *Proc. of 7th COLD METAL FORMING Conference* (Ed. D. Banabic), Cluj Napoca, Romania, pag. 217-224, May 11-12, 2000.
- [29] D. Banabic, H. Aretz, D.S. Comsa, L. Paraianu, An improved analytical description of orthotropy in metallic sheets, *Int. J. Plast.* 21 (2005) 493-512, <https://doi.org/10.1016/j.ijplas.2004.04.003>.
- [30] F. Barlat, J.W. Yoon, O. Cazacu, On linear transformations of stress tensors for the description of plastic anisotropy, *Int. J. Plast.* 23 (5) (2007) 876-896, <https://doi.org/10.1016/j.ijplas.2006.10.001>.
- [31] D.S. Comsa, D. Banabic, *Plane-Stress Yield Criterion for Highly Anisotropic Sheet Metals*, in *Numisheet*, Interlaken, Switzerland, 2008.
- [32] ISO 10113:2006, *Metallic materials — Sheet and strip — Determination of plastic strain ratio*, 2006-09.
- [33] GOM: ARAMIS, *User Information, Software*.
- [34] J.H. Hollomon, *Tensile deformation*, *Trans. Metall. Soc. AIME* 162 (1945) 268-290.
- [35] Shengwen Tu, Xiaobo Ren, Jianying He, Zhiliang Zhang, Stress-strain curves of metallic materials and post-necking strain hardening characterization: a review, *Fatigue Fract. Eng. Mater. Struct.* 43 (1) (2020) 3-19, <https://doi.org/10.1111/ffe.13134>.